Journal of Materials Chemistry

Dynamic Article Links

Cite this: *J. Mater. Chem.*, 2012, **22**, 4575

www.rsc.org/materials

FEATURE ARTICLE

Assemblies of artificial photosynthetic reaction centres

Shunichi Fukuzumi*[ab] and Kei Ohkubo[a]

Received 1st November 2011, Accepted 13th December 2011
DOI: 10.1039/c2jm15585k

Nature harnesses solar energy for photosynthesis in which one reaction centre is associated with a number of light harvesting units. The reaction centre and light-harvesting units are assembled by non-covalent interactions such as hydrogen bonding and π–π interactions. This article presents various strategies to assemble artificial photosynthetic reaction centres composed of multiple light harvesting units and charge-separation units, which are connected by non-covalent bonding as well as covalent bonding. First light-harvesting units are assembled on alkanethiolate-monolayer-protected metal nanoparticles (MNPs), which are connected with electron acceptors by non-covalent bonding. Light-harvesting units can also be assembled using dendrimers and oligopeptides to combine with electron acceptors by π–π interactions. The cup-shaped nanocarbons generated by the electron-transfer reduction of cup-stacked carbon nanotubes have been functionalized with a number of porphyrins acting as light-harvesting units as well as electron donors. In each case, the photodynamics of assemblies of artificial photosynthetic reaction centres have revealed efficient energy transfer and electron transfer to afford long-lived charge-separated states.

1. Introduction

The development of artificial photosynthetic systems using solar energy has been highy desired because of the rising concern of environmental pollution caused by the use of fossil fuels.[1–3] Solar energy has the potential capacity to fulfill global human energy demands in an environmentally benign manner, if efficient, low-cost systems other than natural systems can be developed for making clean fuels such as hydrogen.[1–3] In natural photosynthesis, the photosynthetic reaction centre is associated with a number of light harvesting units in which the harvested light energy is efficiently transferred to the reaction centre where the charge-separation occurs for the primary energy conversion reactions of photosynthesis.[4,5] Extensive efforts have so far been devoted to develop artificial photosynthetic reaction centres, which can mimic the energy and electron-transfer processes in photosynthesis.[6–13] However, covalent syntheses of large molecular arrays are highly inefficient and costly. Thus, an appropriate

[a]*Department of Material and Life Science, Division of Advanced Science and Biotechnology, Graduate School of Engineering, Osaka University, ALCA, Japan Science and Technology Agency (JST), Suita, Osaka, 565-0871, Japan. E-mail: fukuzumi@chem.eng.osaka-u.ac.jp; Fax: +81 6 6879 7370; Tel: +81 6 6879 7368*

[b]*Department of Bioinspired Science, Ewha Womans University, Seoul, 120-750, Korea*

Shunichi Fukuzumi

Shunichi Fukuzumi earned his Ph.D. degree in applied chemistry at Tokyo Institute of Technology in 1978. He has been a Full Professor of Osaka University since 1994. He is the director of an ALCA (Advanced Low Carbon Technology Research and Development) project and the leader of a Global COE program, Global Education and Research Centre for Bio-Environmental Chemistry at Osaka University.

Kei Ohkubo

Kei Ohkubo earned his Ph.D. degree in applied chemistry from Osaka University in 2001. He worked as a JSPS fellow and JST research fellow at Osaka University from 2001 to 2005. He has been a designated associate professor at Osaka University since 2005.

combination of covalent synthesis with the use of non-covalent interactions is required in order to construct functionally integrated ordered architectures from functional building blocks at both the molecular and supramolecular level.

In this article, we would like to focus on recent advancement in construction of hierarchial assemblies of artificial photosynthetic reaction centres by combination of covalent syntheses and the use of a variety of non-covalent interactions. First, nanoparticles are used to assemble artificial photosynthetic reaction centres. Dendrimers, oligopeptides and carbon nanotubes are also utilized to assemble electron donors and acceptors. We have also used a new type of nanocarbon material with controlled size and shape and also porphyrin nanotubes to construct artificial photosynthetic reaction centres. With regard to the lifetime of the charge-separated (CS) state of the artificial photosynthetic reaction centres, a long CS lifetime has been achieved by choosing a suitable chromophore and a redox component.

2. Assemblies on nanoparticles

2.1. Gold nanoparticles

Alkanethiolate-monolayer-protected gold nanoclusters (AuNPs) have merited significant interest, because they provide three dimensional (3D) architectures, which are stable in air and soluble in both nonpolar and polar organic solvents, and also capable of facile modification with other functional thiols through exchange reactions or by couplings and nucleophilic substitutions.[14–19] Thus, AuNPs can be used as excellent materials to assemble artificial photosynthetic reaction centres (*vide infra*).

Extensive studies have so far been done to construct artificial photosynthetic reaction centres starting from dyads, triads, tetrads, and even pentads, which are composed of a chromophore, electron donor(s), and/or acceptor(s), mimicking a multistep photoinduced electron-transfer processes in the photosynthetic reaction centre.[20–25] The multistep photoinduced electron transfer from the spatially defined chromophore to the terminal electron acceptor through a series of electron mediators has well been established to attain fine-tuned and directed redox gradients along donor–acceptor linked arrays for the formation of the long-lived charge-separated state with high efficiency.[20–25] However, such a long-lived CS state has only been attained in compensation for a significant energy loss during the multi-step electron-transfer processes, because each step loses a fraction of the initial excitation energy with the increase in the distance between the positive and negative charges. Instead of using multistep photoinduced electron-transfer processes, one-step photoexcitation of simple electron donor–acceptor dyads has also been reported to afford long-lived CS states.[26–35] Among them, the 9-mesityl-10-methylacridinium ion (Mes–Acr$^+$), which has a small reorganization energy (λ) of electron transfer because the overall charge remains the same in the charge-shift electron transfer, is capable of fast photoinduced electron transfer but extremely slow back electron transfer to form a long-lived electron-transfer state and a π-dimer radical cation between the ground state and electron-transfer state of the dyad.[34] Such a simple molecular dyad capable of fast charge separation, but extremely slow charge recombination, has obvious advantages with regard to synthetic feasibility.[36]

Mes–Acr$^+$ was assembled on AuNPs by a condensation reaction.[36] A carboxylic acid group is introduced in the *N*-methyl group in Mes–Acr$^+$ as shown in Fig. 1.[37] First, *N*-(2-methoxy-ethoxymethyl)-9-acridone (**1**) was synthesized by the reaction of 9(10*H*)-acridone with 2-methoxy-ethoxymethyl chloride. Then, 9-mesitylacridine (**2**) was obtained by the reaction of *N*-protected acridone with 2,4,6-trimethylphenylmagnesium bromide. **2** was reacted with the triflate of benzylglycolate (**3**), which was obtained by the reaction of benzyl glycolate with triflic anhydride to yield 10-benzyloxycarbonylmethyl-9-mesitylacridinium triflate (**4**). Finally the acridinium ester protected by a benzyl group **4** was reacted with hydrogen bromide/acetic acid to yield 10-carboxylmethyl-9-mesitylacridinium hexafluorophosphate (Mes–Acr$^+$–COOH, 43% yield). A reference compound, Mes-Acr$^+$–COOPh, was prepared by condensation of Mes–Acr$^+$–COOH and phenol under similar conditions as described above.

Then, the carboxyl-terminated Mes–Acr$^+$–COOH was directly coupled to 4-mercaptophenol-functionalized Au nanoparticles (PhS-AuNPs) in the presence of *N*,*N*′-diisopropylcarbodiimide (DIPC)[38] and 4-(*N*,*N*-dimethylamino)pyridinium-4-toluenesulfonate (DPTS) as the standard coupling agents as shown in Fig. 2a.[36] The coverage of Mes–Acr$^+$–COOH on the PhS–AuNP was calculated to be 58 molecules per particle (75%).[36] The TEM image (Fig. 2b) revealed the mean diameter of the Au to be 1.7 ± 0.3 nm.[36]

Nanosecond laser flash photolysis measurements of the reference compound (Mes–Acr$^+$–COOH) revealed the transient absorption at 500 nm and a broad absorption band at 1000 nm in the NIR region as shown in Fig. 3a,[36] which are the same as observed in the case of Mes–Acr$^+$.[39] The absorption band at 500 nm was previously assigned to the triplet excited state of the Acr$^+$ moiety.[40,41] However, the absorption band at 500 nm is accompanied by an NIR absorption, which was clearly assigned to the π-dimer radical cation formed between the electron-transfer state (Mes$^{\bullet+}$–Acr$^{\bullet}$) and the ground state of Mes–Acr$^+$.[39]

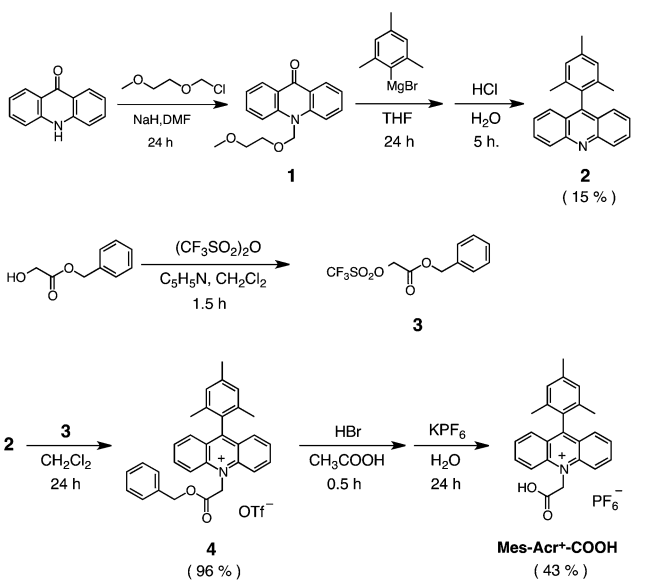

Fig. 1 Synthetic scheme for Mes–Acr$^+$–COOH.

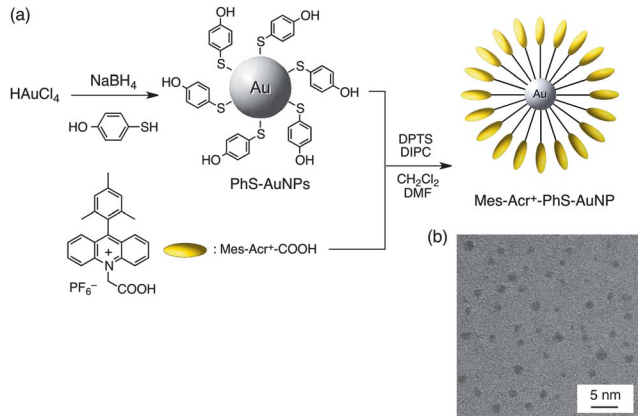

Fig. 2 (a) Synthetic scheme for Mes–Acr$^+$–PhS–AuNP. (b) TEM image of Mes–Acr$^+$–PhS–AuNPs.[36]

The same NIR absorption band was observed in intermolecular photoinduced electron transfer from mesitylene to the singlet excited state of the 10-methylacridinium ion (^{1}AcrH^{+*}).[39] A similar near-IR absorption was also observed for the π-dimer radical cation formed between the electron-transfer state of 2-phenyl-4-(1-naphthyl)quinolinium ion and the ground state.[42,43] Thus, upon photoexcitation of Mes–Acr$^+$–COOPh, the electron transfer state (Mes$^{\bullet+}$–Acr$^\bullet$–COOPh) is formed and then the π-dimer radical cation [(Mes$^{\bullet+}$–Acr$^\bullet$–COOPh)(Mes–Acr$^+$–COOPh)] is formed with Mes–Acr$^+$–COOPh (Scheme 1).[36] Such π-dimer radical cations have been well known to be formed between π-conjugated compounds and the radical cations, which exhibit NIR absorption.[44–46] The decay of the π-dimer radical cation obeyed second-order kinetics, because the intermolecular back electron transfer predominates due to the slow intramolecular back electron transfer as observed in the case of Mes–Acr$^+$.[36]

It should be pointed out that the energy of the acridinium triplet was previously reported to be 1.96 eV, which is lower than the the electron-transfer state (Mes$^{\bullet+}$–Acr$^\bullet$),[40] but this value corresponds to the strong phosphorescence of the corresponding acridine, which remains as an impurity according to the reported synthetic method.[40] It is known that the triplet energy of the acridinium ion is significantly higher than that of the corresponding acridine.[47–49] It should be emphasized that the electron-transfer state (Mes$^{\bullet+}$–Acr$^\bullet$) has both strong oxidizing ability and reducing ability, which enables it to act as an excellent photocatalyst in various photoinducd redox reactions.[50–56]

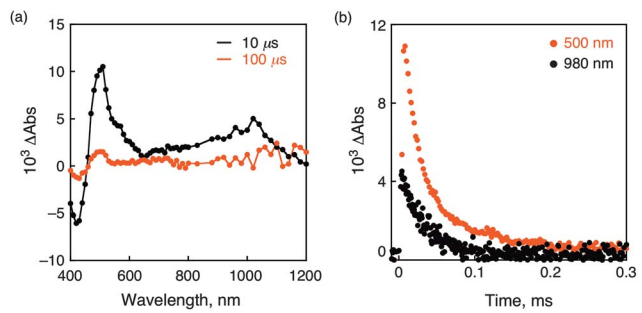

Fig. 3 (a) Transient absorption spectra of Mes–Acr$^+$–COOPh (0.1 mM) in MeCN at room temperature taken 10 μs and 100 μs after nanosecond laser excitation at 430 nm. (b) The time profiles for the decay of Mes$^{\bullet+}$–Acr$^\bullet$–COOPh at 500 nm and 980 nm.

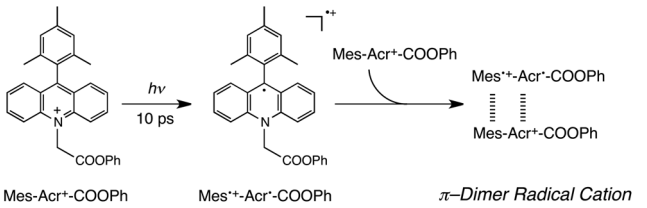

Scheme 1 Photoinduced electron transfer of Mes–Acr$^+$–COOPh and subsequent formation of the π-dimer radical cation.

Femtosecond laser flash photolysis measurements of Mes–Acr$^+$–COOPh with excitation at 420 nm revealed formation of the electron-transfer state as shown in Fig. 4a, where no NIR absorption due to the π-dimer radical cation was observed at 500 ps, because no intermolecular reaction occurred at the time scale in Fig. 4a. In sharp contast to this, femtosecond laser excitation at 420 nm of Mes–Acr$^+$–PhS–AuNPs revealed a transient absorption band at 490 nm together with a broad transient absorption band in the NIR region due to the formation of the π-dimer radical cation of the ET state of Mes–Acr$^+$ (Mes$^{\bullet+}$–Acr$^\bullet$–PhS–AuNPs) with the neighboring Mes–Acr$^+$ molecule. From the distance between two Au atoms (4.06 Å) of the crystal lattice of Au, the distance between two neighboring Mes–Acr$^+$ molecules on the Au surface is estimated to be 8.3 Å.[36] Such close proximity of Mes–Acr$^+$ molecules on the AuNPs makes it possible to form the π-dimer radical cation *via* an intramolecular π–π interaction upon photoinduced electron transfer. The π-dimer radical cation decays with lifetime of 1.9 ps by rapid electron transfer from the benzenethiol linker to the π-dimer radical cation (Mes$^{\bullet+}$–Mes) moiety and back electron transfer to the ground state with the lifetime of 380 ps as shown in the energy diagram in Fig. 5.[36]

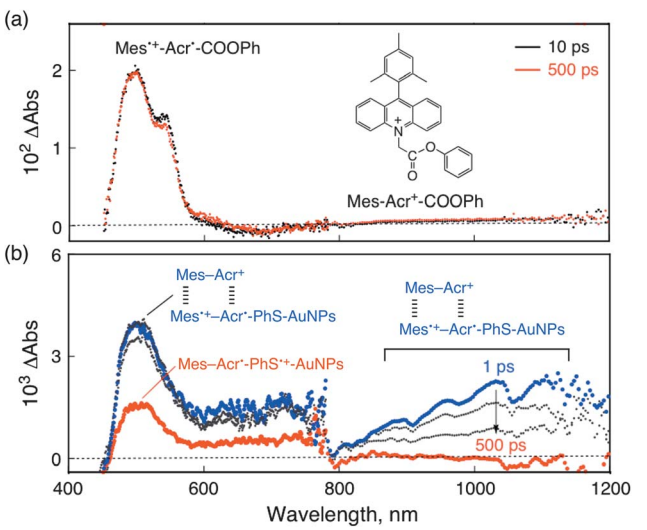

Fig. 4 Transient absorption spectra observed in femtosecond laser flash photolysis (λ_{ex} = 420 nm) of (a) Mes–Acr$^+$–COOPh and (b) Mes–Acr$^+$–PhS–AuNPs in MeCN at 298 K.

Thus, AuNPs provide an excellent scaffold to assemble Mes–Acr$^+$ molecules and the photoexcitation resulted in rapid formation of the electron-transfer state (Mes$^{\bullet+}$–Acr$^{\bullet}$), accompanied by formation of the π-dimer radical cation with the neighbouring Mes–Acr$^+$ on AuNPs, whereas such π-dimer radical cation formation occurs at a much slower time scale for the reference compound (Mes–Acr$^+$–COOPh) by the intermolecular reaction between Mes$^{\bullet+}$–Acr$^{\bullet}$–COOPh and Mes–Acr$^+$–COOPh.

2.2. TiO_2 nanoparticles

Mes–Acr$^+$–COOH and the reference compound (Acr$^+$–COOH) without the donor moiety (Fig. 6) can also be assembled on TiO_2 nanoparticles (TiO_2NPs) by immersing warmed TiO_2NPs (80–100 °C) in an acetonitrile mixture containing Mes–Acr$^+$–COOH and Acr$^+$–COOH for 12 h, respectively.[57] After adsorbing Mes–Acr$^+$–COOH and Acr$^+$–COOH, TiO_2NPs were filtered, and subsequent washing with acetonitrile and drying gave Mes–Acr$^+$–COO–TiO_2NPs and Acr$^+$–COO–TiO_2NPs (Fig. 6).[57] The dye molecule was completely desorbed from the TiO_2NPs into solution by immersing TiO_2NPs modified with the dye moieties in methanol overnight. The amounts of Mes–Acr$^+$–COOH and Acr$^+$–COOH adsorbed on TiO_2NPs relative to the total weight were determined as 1.5×10^{-5} and 1.5×10^{-5} mol g^{-1}, respectively.[57]

Mes–Acr$^+$–COO–TiO_2NPs were electrophoretically deposited onto the OTE/SnO_2 electrode in suspended solution to prepare the OTE/SnO_2/(Mes–Acr$^+$–COO–TiO_2)$_n$ electrode.[57] A mixed cluster suspension of Mes–Acr$^+$–COO–TiO_2 and C_{60} was also prepared in the total concentration range from 0.025 to 0.13 mM (molecular ratio of Mes–Acr$^+$:C_{60} = 1 : 5) in acetonitrile/toluene (3/1, v/v).[57] The clusters suspended in acetonitrile/toluene mixed solvent were assembled electrophoretically as thin films on a conducting glass electrode surface to obtain films of (Mes–Acr$^+$–COO–TiO_2 + C_{60})$_n$ on nanostructured SnO_2 films cast on an optically conducting glass electrode, OTE/SnO_2/(Mes–Acr$^+$–COO–TiO_2 + C_{60})$_n$.[57] A broader wavelength absorption in the visible region was observed in the OTE/SnO_2/(Mes–Acr$^+$–COO–TiO_2 + C_{60})$_n$ film relative to those in the OTE/SnO_2/(Mes–Acr$^+$–COO–TiO_2)$_n$ and OTE/SnO_2/(C_{60})$_n$ films, suggesting the charge-transfer (CT) interaction between Mes–Acr$^+$ moiety and C_{60}.[57]

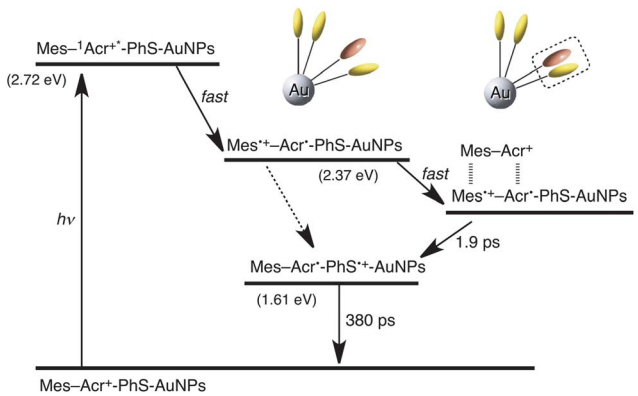

Fig. 5 Energy diagram of photoinduced electron transfer in Mes–Acr$^+$–PhS–AuNPs.

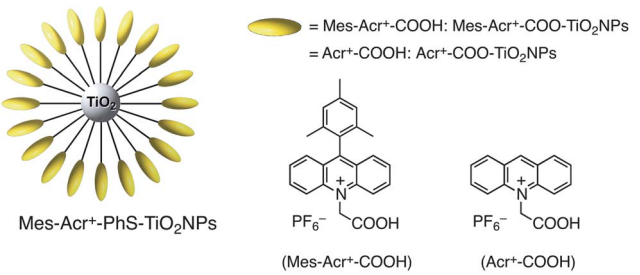

Fig. 6 TiO_2 nanoparticles modified with 9-mesityl-10-carboxymethyl acridinium ion and 10-carboxymethylacridinium ion.

The scanning electron micrograph (SEM) of the OTE/SnO_2/(Mes–Acr$^+$–COO–TiO_2 + C_{60})$_n$ film in Fig. 7 exhibits closely packed clusters of about 20–100 nm size with a networked structure due to a supramolecular interaction between Mes–Acr$^+$–COO–TiO_2 and C_{60} in the TiO_2 nanoparticle matrix.[57] Thus, TiO_2 nanoparticles play an important role in the cluster formation on the films.

Photocurrent measurements of the OTE/SnO_2/(Mes–Acr$^+$–COO–TiO_2 + C_{60})$_n$ electrode as a photoanode in acetonitrile containing NaI (0.5 M) and I_2 (0.01 M) under the bias of 0.2 V *vs.* SCE revealed a significant increase in the photocurrent as compared with those without TiO_2.[57] The incident photon-to-photocurrent efficiency (IPCE) value of 37% was obtained for the OTE/SnO_2/(Mes–Acr$^+$–COO–TiO_2 + C_{60})$_n$ electrode, whereas the maximum IPCE value of the OTE/SnO_2/(Acr$^+$–COO–TiO_2 + C_{60})$_n$ electrode without the electron donor moiety (Mes) was significantly smaller (14%).[57] This indicates that photoinduced electron transfer from the donor moiety (Mes) to the acceptor moiety (Acr$^+$) occurs, followed by electron transfer from the resulting acridinyl radical moiety (Acr$^{\bullet}$) to C_{60} in the supramolecular complex, leading to enhancement of the photocurrent generation.

In the case of the OTE/SnO_2/(Mes–Acr$^+$–COO–TiO_2 + C_{60})$_n$ electrode, the long lifetime of the electron-transfer state (Acr$^{\bullet}$–Mes$^{\bullet+}$) ensures efficient electron-transfer from Acr$^{\bullet}$ to C_{60} (C_{60}/$C_{60}^{\bullet-}$ = −0.2 V *vs.* NHE)[58] to produce the C_{60} radical anion. The formation of $C_{60}^{\bullet-}$ was confirmed by the nanosecond laser flash photolysis measurements of a deoxygenated toluene–acetonitrile (1 : 1, v/v) solution of 9-mesityl-10-methyl-acridinium ion without carboxylic acid (Mes–Acr$^+$)[34] in the presence of C_{60},

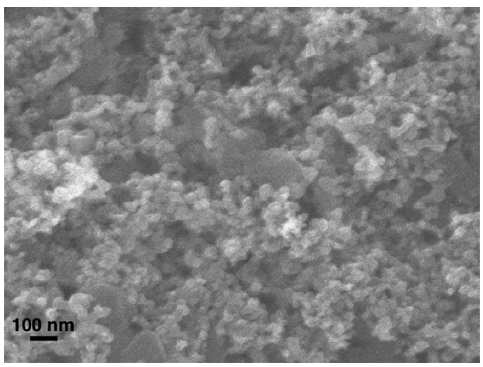

Fig. 7 SEM (scanning electron micrograph) images of OTE/SnO_2/(Mes–Acr$^+$–COO–TiO_2 + C_{60})$_n$ ([Mes–Acr$^+$] = 25 μM, [C_{60}] = 130 μM).

which clearly exhibits a broad absorption band at 1050 nm due to $C_{60}^{\bullet-}$.[59,60] The reduced C_{60} clusters inject electrons into the conduction band of SnO_2, whereas the oxidized mesityl moiety ($Mes^{\bullet+}$) undergoes the electron-transfer reduction with iodide ion in the electrolyte.[57]

2.3. Platinum nanoparticles

Among various metal nanoparticles, Pt nanoparticles (PtNPs) have been known to be the most reactive as hydrogen evolution catalysts.[61] There have been extensive studies on hydrogen evolution using metal complexes as photosensitizers combined with electron mediators and hydrogen-evolution catalysts.[62–67] In order to improve the catalytic efficiency of hydrogen evolution, an electron mediator (methyl viologen) was linked to PtNPs.[68] The methyl viologen-modified platinum clusters (MVA^{2+}–PtNPs) were prepared by applying the same method as the preparation of alkanethiolate-modified AuNPs,[69] as shown in Fig. 8a, where the reduction of H_2PtCl_4 with $NaBH_4$ was performed in water containing MVA^{2+} ($MVA^{2+}/H_2PtCl_4 = 1/1$). The mean diameter of the platinum core ($2R_{CORE}$) of MVA^{2+}–PtNPs determined by transmission electron microscopy (TEM in Fig. 8b) is 1.9 nm (Fig. 8c), which is similar to the diameter reported for the water-soluble PtNPs.[70] The number of MVA^{2+} on the Pt surface is determined to be 67 from the elemental analysis of MVA^{2+}–PtNPs.[68]

MVA^{2+} and MVA^{2+}–PtNPs were reduced by $Na_2S_2O_4$ in aqueous solution at pH 7.0. The formation of a π-dimer radical cation between $MVA^{\bullet+}$ and MVA on PtNPs is recognized in the UV-vis spectrum of $MVA^{\bullet+}$–PtNPs in comparision with that of $MVA^{\bullet+}$ in Fig. 9. The absorption band of $MVA^{\bullet+}$–PtNPs is blue-shifted from 605 nm of $MVA^{\bullet+}$ to 525 nm, accompanied by the appearance of the NIR absorption (Fig. 9b) as observed in the case of the formation of the π-dimer radical cation between $Mes^{\bullet+}$–$Acr^{\bullet}$ and Mes–Acr^{+} in Fig. 3 and 4. This results from closely packed MVA molecules on the Pt surface.[68] The formation of the π-dimer radical cation between $MVA^{\bullet+}$ and MVA^{2+} at close proximity on PtNPs resulted in the positive shift in the first one-electron reduction potential of MVA^{2+}–PtNPs from −0.67 V *vs.* SCE of MVA^{2+} to −0.50 V *vs*. SCE because of the stabilization by the π-bond formed between $MVA^{\bullet+}$ and $MVA^{\bullet+}$.

The hydrogen-evolution efficiency was compared using the photocatalytic systems composed of NADH, Mes–Acr^{+} and MVA^{2+}–PtNPs at pH 4.5 *vs.* NADH, Mes–Acr^{+} and a mixture of the same amounts of MVA^{2+} and PtNPs under the same experimental conditions.[68] The amount of hydrogen evolution of the NADH/Mes–Acr^{+}/MVA^{2+}–PtNPs system increases with the photoirradiation time linearly and the rate was estimated to be 2.4 μmol h^{-1}, which is ten times faster than the rate of the NADH/Mes–Acr^{+}/MVA^{2+}/PtNPs system.[68] The more efficient hydrogen evolution in the NADH/Mes–Acr^{+}/MVA^{2+}–PtNPs system certainly results from the assembly effect of MV^{2+} on PtNPs, which facilitates electron transfer from $MVA^{\bullet+}$ to PtNPs, as compared with intermolecular electron transfer from $MVA^{\bullet+}$ to PtNPs.

Scheme 2 summarizes the mechanism of hydrogen evolution in the NADH/Mes–Acr^{+}/MVA^{2+}–PtNPs system.[68] The photocatalytic hydrogen evolution starts by photoexcitation of Mes–Acr^{+}, which results in the formation of the electron-transfer

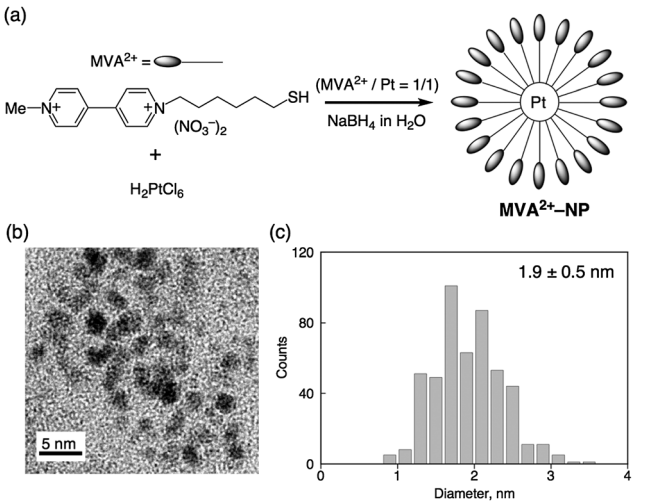

Fig. 8 (a) Preparation of MVA^{2+}–PtNPs. (b) Transmission electron microscopy (TEM) image and (c) core size histograms of MVA^{2+}–PtNPs.

state ($Acr^{\bullet}$–$Mes^{\bullet+}$). This is followed by the rapid electron-transfer oxidation of NADH and/or the electron-transfer reduction of MVA^{2+} in MVA^{2+}–PtNPs. Both processes are thermodynamically feasible, because the one-electron oxidation potential of NADH (E_{ox} = 0.76 V *vs.* SCE)[71,72] is less positive than the one-electron reduction potential of the $Mes^{\bullet+}$ moiety of $Mes^{\bullet+}$–Acr and the one-electron oxidation potential of the $Acr^{\bullet}$ moiety in water ($E_{ox} = -0.57$ V *vs.* SCE) is more negative than the one-electron reduction potential of the MVA^{2+} moiety in MVA^{2+}–PtNPs ($E^0_{red} = -0.50$ V). In contrast, electron transfer from $Acr^{\bullet}$–$Mes^{\bullet+}$ ($E_{ox} = -0.57$ V *vs.* SCE) to MV^{2+} ($E_{red} = -0.67$ V) is energetically unfavorable, because the E_{ox} value of $Mes^{\bullet+}$–$Acr^{\bullet}$ is more positive than the E^0_{red} value of MV^{2+}. In this case, MV^{2+} is reduced by $NAD^{\bullet}$, which is produced *via* deprotonation of $NADH^{\bullet+}$, because the electron transfer from $NAD^{\bullet}$ ($E_{ox} = -1.1$ V *vs.* SCE)[71,72] to MV^{2+} ($E_{red} = -0.67$ V) is highly exergonic. Thus, MVA^{2+}–PtNPs are more reactive in electron transfer from $Mes^{\bullet+}$–$Acr^{\bullet}$ and also electron transfer to PtNPs, leading to the 10 times faster H_2 evolution.

2.4. Porphyrin assembled metal nanoparticles

In order to expand the potential applications of metal nanoparticles (MNPs), systematic studies on chromophore-modified

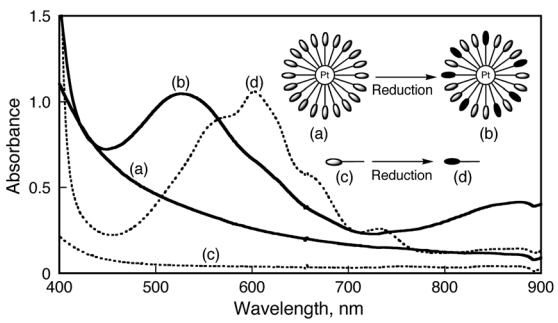

Fig. 9 UV-vis spectra of (a) MVA^{2+}–PtNPs, (b) $MVA^{\bullet+}$–PtNPs, (c) MVA^{2+} and (d) $MVA^{\bullet+}$ in aqueous solution at pH 7.0.

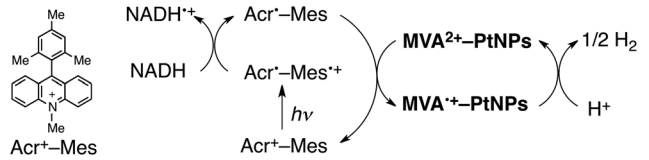

Scheme 2 Catalytic cycle of hydrogen evolution from NADH and water with Mes–Acr^+ and MVA^{2+}–PtNPs.

MNPs are required. Brust *et al.* developed a facile synthetic method in which a quaternary ammonium salt is used to assist the transfer of gold ion [$(AuCl_4)^-$] and reducing agent (BH_4^-) from aqueous phase to organic phase to yield air-stable functionalized MNPs with a mono dispersity.[14] This method was utilized to prepare porphyrin-modified metal nanoclusters with different metal and different size of gold core (H_2PC11AuNPs, H_2PC11AuNPs, H_2PC11AuNPs, H_2PC11PdNPs, H_2PC11PtNPs, H_2PC11Au/AgNPs), as shown in Fig. 10.[73]

The different size of metal core was obtained by changing the concentraion of porphyrin alkanethiol (Por-SH) as shown in the TEM images of H_2PC11AuNPs (Fig. 11).[73] Based on the elemental analysis, there are 25, 57 and 136 porphyrin alkanethiolate chains on the gold surface for H_2PC11AuNPs with the mean diameter $2R_{CORE} = 1.4$ nm, 2.1 and 2.9 nm, respectively.[19] The coverage ratios of porphyrin alkanethiolate chains of H_2PC11AuNPs with $2R_{CORE} = 1.4$ nm, 2.1 and 2.9 nm to surface Au atoms (γ) were determined to be 46%, 40% and 46%, respectively. These γ values are remarkably large compared with the coverage ratio ($\gamma = 6.5\%$) of 2D porphyrin SAM H_2PC11–Au(111).[74] Such enhanced packing of the large porphyrins is made possible by the highly curved outermost surface of the AuNPs, where the spacer is splayed outward from the gold core to relieve steric crowding significantly. Similar results were obtained for H_2PC11Au/AgNPs, H_2PC11PdNPs and H_2PC11PtNPs.[73]

Although there are many porphyrins attached on MNPs, there is no significant interaction between porphyrin molecules on MNPs, because the λ_{max} values of the Soret band of H_2PC11MNPs in benzene, THF and $CHCl_3$ are nearly identical to that of Por-ref in the three solvents. The surface plasmon absorption due to the gold,[75] palladium,[76] platinum[70b] and alloy gold–silver[77] nanoparticles is much weaker than that of the porphyrin moiety.

Fluorescence lifetimes of H_2PC11AuNPs with $2R_{CORE} =$ 1.4 nm, 2.1 and 2.9 nm were determined to be 0.17 ns (97%), 0.10 ns (96%), 0.12 ns (73%), respectively.[73] The similar quenching efficiency reveals that the difference in metal size (1.4 nm–2.9 nm) has no appreciable impact on the quenching of the porphyrin excited singlet state by the metal surfaces. It should be noted that the fluorescence lifetime of H_2PC11Au/AgNPs [0.22 (81%) and 7.0 ns (19%) in $CHCl_3$ ($\lambda_{obs} = 720$ nm)] is significantly longer than those of monometal H_2PC11AuNPs.[73] This suggests that interaction between the surface of the gold-silver alloy and the porphyrin excited singlet state is attenuated considerably relative to the mono-metal systems. Thus, porphyrin-modified metal alloy nanoclusters are highly promising as new types of light-harvesting materials, photocatalysts, and chemical and biochemical sensors.[78]

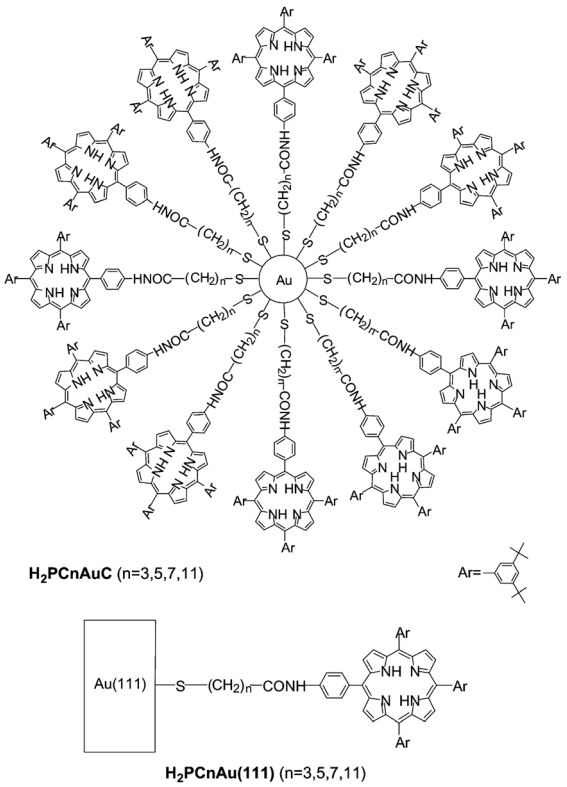

Fig. 10 Schematic structures of porphyrin-modified gold nanoclusters H_2PC*n*AuNPs.

These porphyrin-modified MNPs form π-complexes with fullerene molecules and they were clusterized in an acetonitrile/toluene mixed solvent.[79] Then, the highly colored composite clusters were assembled as a three-dimensional array onto nanostructured SnO_2 films to afford the OTE/SnO_2/(H_2PC*n*MNPs + C_{60})$_m$ electrode (*n* is the number of alkyl chains) using an electrophoretic deposition method.[79] The film of the composite cluster with gold nanoparticle exhibits an incident

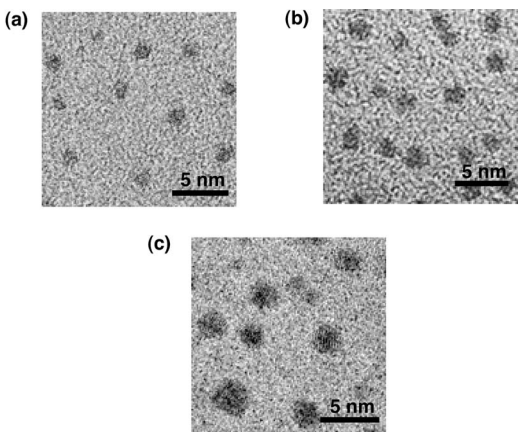

Fig. 11 Transmission electron microscopy (TEM) images of H_2PC11AuNPs with different sizes; (a) $2R_{CORE} = 1.4$ nm with a standard deviation ($\sigma = 0.4$ nm), (b) $2R_{CORE} = 2.1$ nm with $\sigma = 0.3$ nm and (c) $2R_{CORE} = 2.9$ nm with $\sigma = 0.7$ nm. The dark spots correspond to the metal core.

photon-to-photocurrent efficiency (IPCE) as high as 54% and broad photocurrent action spectra (up to 1000 nm).[79] The energy conversion efficiency of this system reaches 1.5%, and this value is 45 times higher than that of the reference system.[79] Such remarkable enhancement in the photoelectrochemical performance as well as broader photoresponse in the visible and infrared relative to the reference systems demonstrates that the porphyrin-AuNPs and fullerene composites provide promising perspective for the development of efficient organic solar cells.

3. Dendrimer supramolecular complexes

Because the morphology and the photochemical function of porphyrin dendrimers are similar to those of the light-harvesting units in photosynthesis, porphyrin dendrimers have attracted considerable interest as a unique way to assemble porphyrins, harvesting solar light in artificial photosynthesis.[80–83] Porphyrin dendrimers can also be used to combine light-harvesting units with reaction centre units. For example, a zinc porphyrin dendrimer $[D(ZnP)_{16}]$[84] is combined with an electron acceptor, *N*-methyl-2-(4′-pyridyl)-3,4-fulleropyrrolidine (PyC_{60}), which has a pyridine binding site,[85] to form a supramolecular complex as shown in Fig. 12.[86] The porphyrin dendrimers were synthesized by coupling of the porphyrin activated ester [5-amino-2-{5,10,15,20-tetrakis(3,5-di-*tert*-butylphenyl)}]-5-oxopentanoic acid 2,5-dioxopyrrolidin-1-yl ester with the appropriate first, second, or third generation polypropylenimine dendrimer.[83]

Photoexcitation of the Soret band of $D(ZnP)_{16}$ at 438 nm in PhCN results in fluorescence at $\lambda_{max} = 609$ and 645 nm.[11b] The fluorescence was efficiently quenched by addition of PyC_{60} to a PhCN solution of $D(ZnP)_{16}$.[11b] The fluorescence intensity decreases to reach a constant value with increasing concentration of PyC_{60}. The formation constant (K) of 1 : 1 ZnP monomer unit–PyC_{60} complex was determined from the fluorescence quenching to be 5.0×10^4 M^{-1}, which is significantly larger than the K value (1.6×10^4 M^{-1}) determined from the absorption spectral change.[11b] The larger K value determined from the fluorescence quenching results from the excited energy migration between the porphyrin units, because the fluorescence of the unbounded ZnP moiety is quenched by PyC_{60} bound to a different ZnP moiety *via* the energy transfer. In contrast to the case of $D(ZnP)_{16}$, a ZnP monomer cannot form the supramolecular complex with PyC_{60} in a coordinating PhCN solution, when no fluorescence quenching occurred by PyC_{60}.[11b] This indicates clearly that the dendrimer affects the binding and excited energy migration.

The occurrence of photoinduced charge separation (CS) in the supramolecular complex was confirmed by nanosecond laser flash photolysis measurements of the $D(ZnP)_{16}$–PyC_{60} complex in PhCN as shown in Fig. 13.[11b] The absorption band due to $PyC_{60}^{\bullet-}$ is clearly observed at 1000 nm together with that due to $ZnP^{\bullet+}$ at 630 nm after laser excitation at 561 nm where only the ZnP moiety is excited (Fig. 13a).[11b] This indicates that the CS state of the supramolecular complex is formed *via* photoinduced electron transfer from the singlet excited state of the ZnP moiety to the PyC_{60} moiety. The quantum yield (Φ) of the CS state of the $D(ZnP)_{16}$–PyC_{60} complex is determined to be 25%.[11b] The decay of the absorption band at 1000 nm due to $PyC_{60}^{\bullet-}$ obeyed clean first-order kinetics with the same slope irrespective of different laser power intensities (Fig. 13b).[11b] Because intermolecular back electron transfer would obey second-order kinetics, the first-order decay of the CS state results from back electron transfer in the supramolecular complex. The lifetime of the CS state is determined as 0.25 ms at 298 K.[11b]

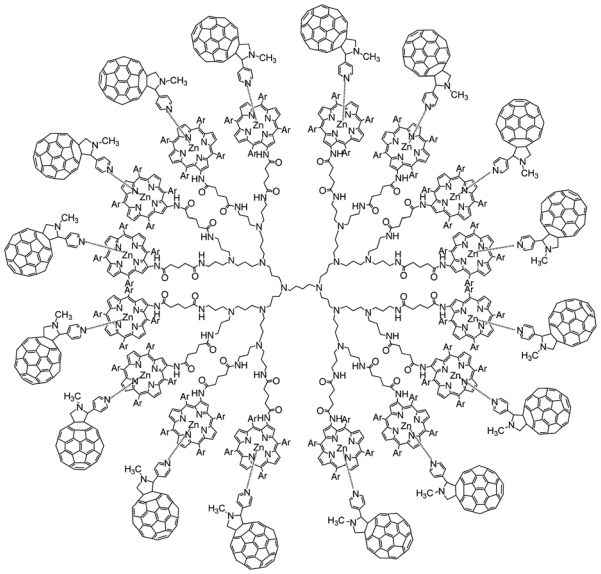

Fig. 12 A supramolecular complex between a zinc porphyrin dendrimer $[D(ZnP)_{16}]$ and PyC_{60}.

Organic photovoltaic cells were constructed using clusters of supramolecular complexes of porphyrin dendrimers with fullerene exhibiting remarkable enhancement in the photoelectrochemical performance as well as broader photoresponse in the visible and near-infrared regions.[84,86] This clearly indicates that the π–π interaction between porphyrins and fullerenes in the supramolecular clusters plays an important role in improving the light energy conversion efficiency.

4. Porphyrin oligopeptide supramolecular complexes

In contrast to porphyrin dendrimers (Fig. 12) in which the geometries of porphyrins are rather fixed, porphyrin

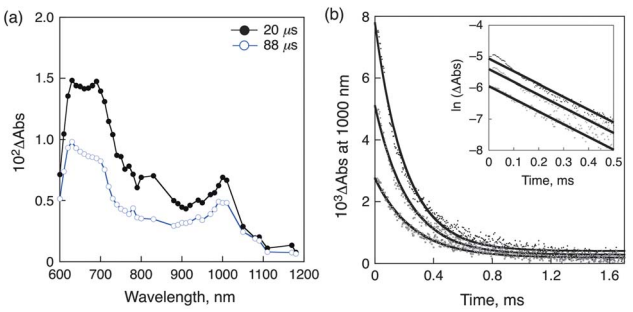

Fig. 13 (a) Transient absorption spectra of $D(ZnP)_{16}$ (2.3×10^{-5} M) in the presence of PyC_{60} (5.2×10^{-5} M) in deaerated PhCN at 298 K taken at 20 μs (solid line with black circles) and 88 μs (solid line with white circles) after laser excitation at 561 nm, respectively. (b) Time profiles of the absorption at 1000 nm of $PyC_{60}^{\bullet-}$ with different laser intensities (3.0, 1.0, and 0.5 mJ/pulse) at 298 K. Inset: First-order plots.

oligopeptides provide more flexible structures to assemble porphyrins.[87,88] Thus, zinc porphyrinic oligopeptides with various numbers of porphyrin units [$P(ZnP)_n$; $n = 2, 4, 8$][87–89] are used as light-harvesting multiporphyrin units, which are bound to electron acceptors of fulleropyrrolidine bearing a pyridine (PyC_{60})[85,90] or imidazole coordinating ligand (ImC_{60})[91] as shown in Fig. 14.[92]

The fluorescence of $P(ZnP)_8$ is strongly quenched by the intrasupramolecular electron transfer from the singlet excited state of the ZnP moiety ($^1ZnP^*$) in $P(ZnP)_8$ to the bound PyC_{60}.[92] The formation constant (K) of the supramolecular complex of $P(ZnP)_8$ with PyC_{60} was determined from the fluorescence quenching to be 1.5×10^5 M^{-1}, which is significantly larger than the K value (2.4×10^4 M^{-1}) determined from the absorption spectral change.[92] As in the case of the supramolecular complex of zinc porphyrin dendrimers with PyC_{60} (*vide supra*), the larger K value determined from the fluorescence quenching results from the excited energy migration between the porphyrin units in $P(ZnP)_8$. It should be noted that the K value determined from the fluorescence quenching of $P(ZnP)_8$ by PyC_{60} (1.5×10^5 M^{-1}) is significantly larger than the corresponding value of $D(ZnP)_{16}$ (5.0×10^4 M^{-1}) but that the K values determined from the absorption spectral change are similar between $P(ZnP)_8$ and $D(ZnP)_{16}$.[92] This suggests that the flexible structure of the oligopeptide chain enables more efficient energy migration as compared with the rigid structure of the dendrimer. The flexibility of the oligopeptide chain was clearly observed as the disappearance of the Cotton effect originating from the porphyrin Soret band at 428 nm in the circular dichroism (CD) spectra of $P(ZnP)_{16}$ by the formation of the supramolecular complex with C_{60}, which indicates the α-helix structure was changed to accommodate C_{60} between the porphyrin rings by π–π interaction.[93]

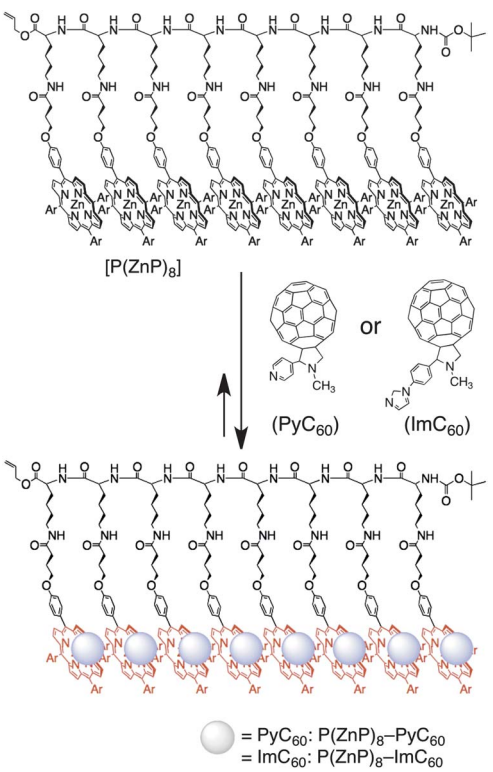

Fig. 14 Supramolecular complex composed of the porphyrin–peptide octamer [$P(ZnP)_8$, Ar = 3,5-(*tert*-Bu)$_2C_6H_3$] and PyC_{60} or ImC_{60}.

As in the case of the $D(ZnP)_{16}$–PyC_{60} supramolecular complex in Fig. 13a, the occurrence of photoinduced electron transfer in the supramolecular complex in PhCN was confirmed by nanosecond laser flash photolysis measurements of the supramolecular complex of $P(ZnP)_8$ with PyC_{60}, which revealed the formation of the CS state, exhibiting the transient absorption band due to $PyC_{60}^{\bullet-}$ at 1000 nm together with that due to $ZnP^{\bullet+}$ at 630 nm.[92] The CS state decayed obeyed clean first-order kinetics and the first-order plots at different initial CS concentrations afforded linear correlations with the same slope. If there is any contribution of intermolecular back electron transfer from unbound $PyC_{60}^{\bullet-}$ to $ZnP^{\bullet+}$, the second-order kinetics would be involved for the decay time profile. Thus, the decay of the CS state results from back electron transfer in the supramolecular complex rather than intermolecular back electron transfer from $PyC_{60}^{\bullet-}$ to $ZnP^{\bullet+}$.[92]

The CS lifetimes of the supramolecular complexes of other porphyrins [$P(ZnP)_n$: $n = 2, 4$] and fullerene derivative (ImC_{60}) become longer with increasing generation of porphyrinic oligopeptides.[92] This may also result from efficient hole migration between the porphyrin units following photoinduced electron transfer in the supramolecular complex. The longest CS lifetime was attained as 0.84 ms at 298 K for the $P(ZnP)_8$–ImC_{60} supramolecular complex.[92] Such a long-lived CS state was also confirmed by the EPR measurements under photoirradiation of the supramolecular complexes of $P(ZnP)_8$ with PyC_{60} and ImC_{60} in frozen PhCN at 173 K. Under photoirradiation, the isotropic EPR signals corresponding to the zinc porphyrin radical cation and fullerene radical anion were observed at $g = 2.002$ and 2.000, respectively.[92]

The clusters of supramolecular complexes of porphyrin-peptide oligomers with fullerenes can be assembled on nanostructured SnO_2 electrodes by an electrophoretic deposition method to construct purely organic supramolecular solar cells.[93] There were significant effects of the number of porphyrins in a poly-peptide unit [$P(H_2P)_n$ and $P(ZnP)_n$ ($n = 1$, 2, 4, 8, 16)] and of the types of porphyrins (H_2P *vs.* ZnP) and fullerenes (C_{60} *vs.* C_{60} derivatives) on the structures, spectroscopic, and photoelectrochemical properties of the porphyrin–C_{60} composite electrodes.[93] The best performance was obtained for the $(P(H_2P)_{16} + C_{60})_m$ system exhibiting a fill factor (FF) of 0.47, an open circuit voltage (V_{oc}) of 320 mV, a short circuit current density (I_{sc}) of 0.36 mA cm^{-2}, and the overall power conversion efficiency (η) of 1.6% at input power (W_{in}) of 3.4 mW cm^{-2}, which is 40 times higher than the value (0.043%) of the porphyrin monomer $(P(H_2P)_1 + C_{60})_m$ modified electrode.[93b] The broad photocurrent action spectra (with photoresponse extending up to 1000 nm) show the ability of these composites to harvest photons in the visible and NIR. Thus, a supramolecular approach between porphyrins and fullerenes with flexible polypeptide structures seems to be promising, making it possible to further improve the light energy conversion effciency by using a much larger number of porphyrins in a polypeptide unit.

5. Porphyrin assembly on size-controlled cup-shaped nanocarbons

In addition to fullerenes described above, single-walled carbon nanotubes (SWNTs)[94] also exhibit excellent chemical and physical properties that have been revealed by various potential applications.[95–99] Thus, extensive efforts have so far been devoted to assemble electron donor and acceptor molecules on SWNTs.[7,100–106] However, the fine-control of size (*i.e.*, length) of SWNTs remains a formidable challenge, because SWNTs have seamless cylinder structures made up of a hexagonal carbon network, which leads to the difficulty of solubilisation/functionalization without treatment of strong acid or vigorous sonication.[107,108] On the other hand, the cup-stacked carbon nanotubes (CSCNTs) that consist of cup-shaped nanocarbon units, which stack *via* van der Waals attractions, have merited special attention from the viewpoint of conventional carbon nanotube alternatives.[109–112] The tube-tube van der Waals energy between cup-shaped nanocarbons has been counterbalanced by the thermal or photoinduced electron transfer multi-electron reduction due to electrostatic repulsion, resulting in highly dispersible cup-shaped nanocarbons with size homogeneity.[113,114]

The cup-shaped nanocarbons (CNC) with controlled size have been functionalized with a large number of porphyrin molecules.[115] The general procedure for the synthesis of the porphyrin-functionalized cup-shaped nanocarbons [CNC–$(H_2P)_n$] is shown in Fig. 15a.[115] The cup-shaped nanocarbons are first functionalized with aniline as the precursor for the further functionalization with porphyrins. The aniline-functionalized nanocarbons react with the porphyrin derivatives to construct the nanohybrids.

The structure of the cup-shaped nanocarbons of the CNC–$(H_2P)_n$ nanohybrids is shown by the TEM in Fig. 15b, which reveals cup-shaped nanocarbons with a hollow core along the length of the nanocup with well-controlled diameter (*ca.* 50 nm) and size (*ca.* 100 nm).[114] The weight % of porphyrins attached to the cup-shaped nanocarbons was determined by thermogravimetric analysis (TGA) and elemental analysis to be *ca.* 20%.[114] This corresponds to one functional group per 640 carbon atoms of the nanocup framework for the CNC–$(H_2P)_n$ nanohybrid. Thus, the π-framework of the CNC is not destroyed despite attachment of a large number of porphyrin molecules on the CNC.

Spectroscopic evidence for the covalent functionalization of the CNC–$(H_2P)_n$ nanohybrid was obtained by an intensity increase of the Raman signal at 1353 cm^{-1} (D band) in the functionalized CNC as compared with the pristine CSCNTs,[115] because the D band has been used for monitoring the process of functionalization which transforms sp^2 to sp^3 sites.[116] The UV-vis absorption spectrum of the CNC–$(H_2P)_n$ nanohybrid agreed with that of the superposition of the reference porphyrin [tetrakis(*N*-octadecyl-4-aminocarboxyphenyl)porphyrin] (ref-H_2P) and cup-shaped nanocarbons, indicating that there is no significant interaction between attached porphyrins and CSCNTs in the ground states.[115]

The fluorescence lifetime of CNC–$(H_2P)_n$ was determined to be 3.0 ± 0.1 ns, which is much shorter than that of ref-H_2P (14.1 ± 0.1 ns).[115] The fluorescence emission at 650 nm was also quenched in CNC–$(H_2P)_n$.[115] The short fluorescence lifetime of

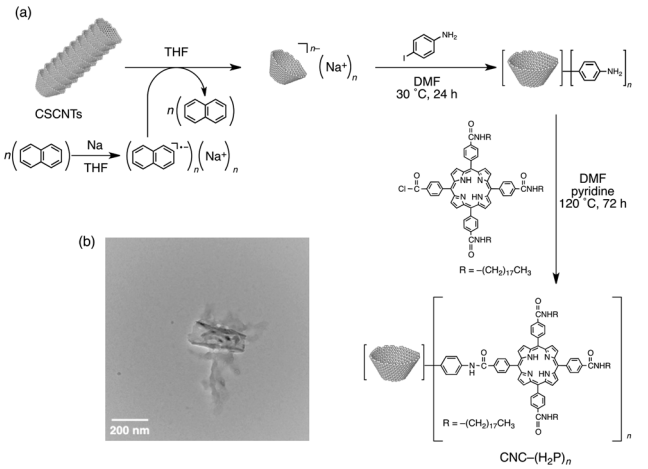

Fig. 15 (a) Synthetic procedure of CNC–$(H_2P)_n$. (b) TEM image of CNC–$(H_2P)_n$.

CNC–$(H_2P)_n$ and an efficient fluorescence quenching of porphyrins in CNC–$(H_2P)_n$ as compared to the ref-H_2P may result from the photoinduced electron transfer from the singlet excited state of H_2P ($^1H_2P^*$) to CNC in CNC–$(H_2P)_n$. The occurrence of the photoinduced electron transfer to afford the charge-separated (CS) state of CNC–$(H_2P)_n$ was confirmed by

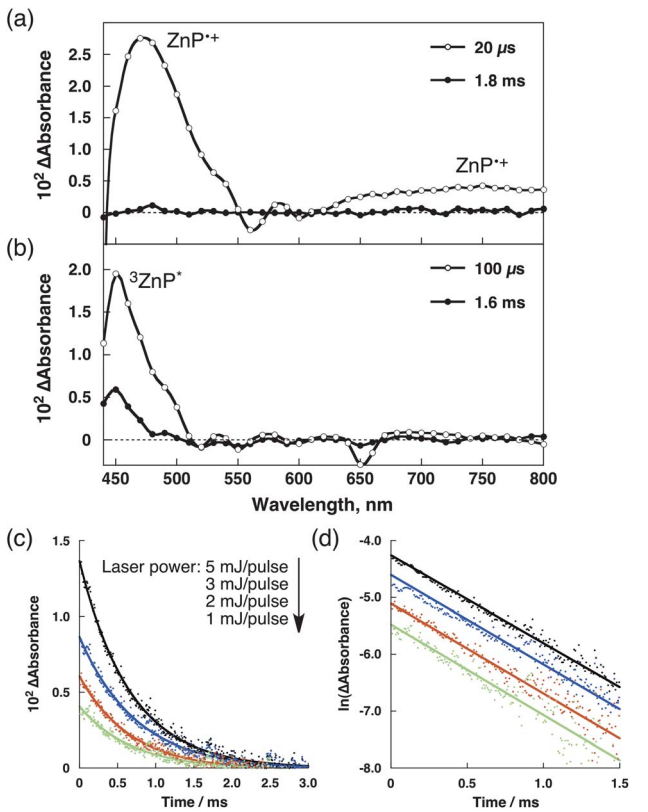

Fig. 16 (a) Transient absorption spectra of (a) CNC–$(H_2P)_n$ taken at 20 μs and 1.8 ms after laser excitation at 426 nm and (b) ref-H_2P in deaerated DMF at 298 K taken at 100 μs and 1.6 ms after laser excitation at 426 nm. (c) Decay time profiles and (d) first-order plots at 470 nm with different laser powers (5, 3, 2, and 1 mJ/pulse).

nanosecond laser flash photolysis measurements in Fig. 16, where the absorption bands in the visible and NIR region are attributed to $H_2P^{\bullet+}$, which are clearly different from the triplet–triplet absorption of ref-H_2P.[115] The formation of the CS state was also confirmed by EPR measurements under photoirradiation of CNC–$(H_2P)_n$ in frozen DMF at 153 K. The observed isotropic EPR signal at $g = 2.0044$ agrees with that of ref-$H_2P^{\bullet+}$ produced by the one-electron oxidation with $[Ru(bpy)_3]^{3+}$ (bpy = 2,2′-bipyridine) in deaerated $CHCl_3$.[115] The EPR signal corresponding to the reduced carbon-based nanomaterials was too broad to be detected probably due to delocalization of electrons in CNC.[115]

The CS state of CNC–$(H_2P)_n$ detected in Fig. 16a decays obeying clean first-order kinetics: the first-order plots at different initial CS concentrations afford linear correlations with the same slope (Fig. 16b).[115] Thus, the decay of the CS state results from back electron transfer in the nanohybrid rather than intermolecular back electron transfer from $CNC^{\bullet-}$ to $H_2P^{\bullet+}$. The CS lifetime was determined from the first-order plots in Fig. 16b to be 0.64 ± 0.01 ms, which is the longest lifetime ever reported for electron donor-attached nanocarbon materials.[115] Such a long CS lifetime may be ascribed to the efficient electron migration in the cup-shaped nanocarbons following the charge separation.

The reduction potential (E_{red}) of the CNC moiety was estimated by redox titration to be −0.15 V *vs.* SCE,[115] which is about the same as the reported value of the one-electron reduction potential of CNT.[117] In the presence of TCNQ ($E_{red} = 0.19$ V *vs.* SCE), which acts as an electron acceptor, photoinduced electron transfer from H_2P to CNC in CNC–$(H_2P)_n$ was followed by subsequent electron transfer from $CNC^{\bullet-}$ of the CS state to TCNQ to produce $TCNQ^{\bullet-}$ (λ_{max} = 846 nm), whereas the absorption bands due to $H_2P^{\bullet+}$ at 480 nm and the near-infrared region remain the same as shown in Fig. 17.[115] This serves as crucial testimony for the existence of the photolytically generated $CNC^{\bullet-}$ (*i.e.*, $CNC^{\bullet-}$–$(H_2P)_n^{\bullet+}$).

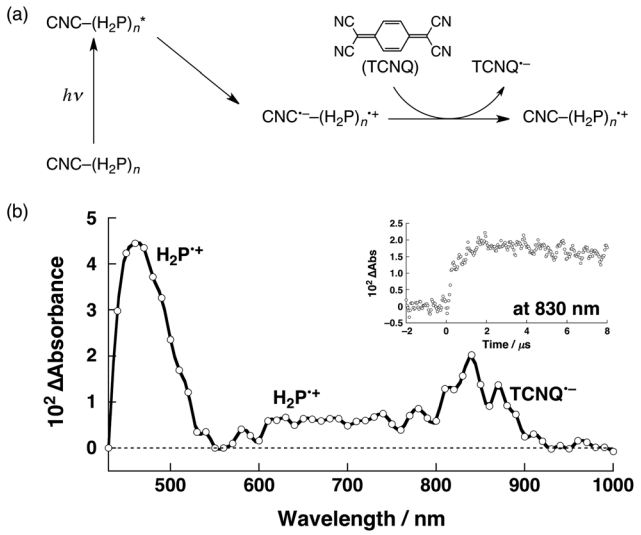

Fig. 17 (a) Reaction course of photoinduced charge separation of CNC–$(H_2P)_n$ and electron-transfer reduction of TCNQ with the CS state. (b) Transient absorption spectrum recorded at 1 μs after 426 nm laser excitation of a deaerated DMF solution of CNC–$(H_2P)_n$ in the presence of TCNQ (1.0×10^{-6} M). Inset: Absorption-time profile recorded at 830 nm.

Porphyrin-functionalized cup-shaped nanocarbons CNC–$(H_2P)_n$ have also been assembled onto nanostructured SnO_2 films using an electrophoretic deposition method to examine the photoelectrochemical properties.[118] The resulting nanohybrid film afforded the drastic enhancement in the photoelectrochemical performance as well as the broader photoresponse in the visible region as compared with the reference CNC system without porphyrins.[119] The enhancement of photocurrent generation is caused by the efficient electron injection from the long-lived charge-separated state of CNC–$(H_2P)_n$ upon photoexcitation (*vide supra*).

6. Conclusions

In contrast to natural photosynthesis, where only a single reaction centre is combined with light-harvesting units, multiple reaction centres can be combined with light-harvesting units by utilizing metal nanoparticles, dendrimers, oligopeptides and nanocarbon materials, in which charge-separation molecules are assembled in artificial systems as described above. The construction of composites of multiple photosynthetic reaction centres and light-harvesting units described in this article will hopefully open a new strategy to develop efficient light-to-energy conversion systems including organic solar cells and artificial photosynthesis for production of solar fuels.

Acknowledgements

The authors gratefully acknowledge the contributions of their collaborators and coworkers mentioned in the cited references, and support by a Grant-in-Aid (Nos. 20108010 and 237500141), a Global COE program, "the Global Education and Research Center for Bio-Environmental Chemistry" from the Ministry of Education, Culture, Sports, Science and Technology, Japan and KOSEF/MEST through WCU project (R31-2008-000-10010-0), Korea.

References

1 (*a*) H. B. Gray, *Nat. Chem.*, 2009, **1**, 7; (*b*) J. L. Dempsey, B. S. Brunschwig, J. R. Winkler and H. B. Gray, *Acc. Chem. Res.*, 2009, **42**, 1995.
2 (*a*) N. S. Lewis and D. G. Nocera, *Proc. Natl. Acad. Sci. U. S. A.*, 2006, **103**, 15729; (*b*) V. Balzani, A. Credi and M. Venturi, *ChemSusChem*, 2008, **1**, 26–58; (*c*) S. Fukuzumi, *Eur. J. Inorg. Chem.*, 2008, **9**, 1351.
3 (*a*) D. L. Royer, R. A. Berner and J. Park, *Nature*, 2007, **446**, 530; (*b*) Y. Pellegrin and F. Odobel, *Coord. Chem. Rev.*, 2011, **255**, 2578.
4 (*a*) *Anoxygenic Photosynthetic Bacteria*, ed. R. E. Blankenship, M. T. Madigan and C. E. Bauer, Kluwer Academic Publisher, Dordecht, 1995; (*b*) *The Photosynthetic Reaction Center*, ed. J. Deisenhofer and J. R. Norris, Academic Press, San Diego, 1993; (*c*) *Molecular Level Artificial Photosynthetic Materials*, ed. G. J. Meyer, Wiley, New York, 1997.
5 (*a*) R. A. Wheeler, in *Introduction to the Molecular Bioenergetics of Electron, Proton, and Energy Transfer*, ACS Symposium Ser, 2004, Vol. 883, 1–6; (*b*) W. Leibl and P. Mathis, in *Electron Transfer in Photosynthesis.* Series on Photoconversion of Solar Energy, 2004, Vol. 2, 117.
6 (*a*) D. Gust, T. A. Moore and A. L. Moore, *Acc. Chem. Res.*, 2001, **34**, 40; (*b*) D. Gust, T. A. Moore and A. L. Moore, *Acc. Chem. Res.*, 2009, **42**, 1890.
7 (*a*) D. M. Guldi, G. M. A. Rahman, F. Zerbetto and M. Prato, *Acc. Chem. Res.*, 2005, **38**, 871; (*b*) G. Bottari, G. de la Torre, D. M. Guldi

and T. Torres, *Chem. Rev.*, 2010, **110**, 6768; (*c*) V. Sgobba and D. M. Guldi, *Chem. Soc. Rev.*, 2009, **38**, 165.
8 (*a*) M. R. Wasielewski, *Chem. Rev.*, 1992, **92**, 435; (*b*) M. R. Wasielewski, *Acc. Chem. Res.*, 2009, **42**, 1910.
9 (*a*) S. Fukuzumi, *Org. Biomol. Chem.*, 2003, **1**, 609; (*b*) S. Fukuzumi, *Bull. Chem. Soc. Jpn.*, 2006, **79**, 177; (*c*) S. Fukuzumi, *Phys. Chem. Chem. Phys.*, 2008, **10**, 2283.
10 (*a*) F. D'Souza and O. Ito, *Chem. Commun.*, 2009, 4913; (*b*) F. D'Souza and O. Ito, *Coord. Chem. Rev.*, 2005, **249**, 1410; (*c*) S. Fukuzumi and T. Kojima, *J. Mater. Chem.*, 2008, **18**, 1427.
11 (*a*) M.-S. Choi, T. Yamazaki, I. Yamazaki and T. Aida, *Angew. Chem., Int. Ed.*, 2004, **43**, 150; (*b*) S. Fukuzumi, K. Saito, K. Ohkubo, T. Khoury, Y. Kashiwagi, M. A. Absalom, S. Gadde, F. D'Souza, Y. Araki, O. Ito and M. J. Crossley, *Chem. Commun.*, 2011, **47**, 7980.
12 (*a*) T. Kojima, T. Honda, K. Ohkubo, M. Shiro, T. Kusukawa, Fukuda, N. Kobayashi and S. Fukuzumi, *Angew. Chem., Int. Ed.*, 2008, **47**, 6712; (*b*) S. Fukuzumi, T. Honda, K. Ohkubo and T. Kojima, *Dalton Trans.*, 2009, 3880; (*c*) T. Kojima, K. Hanabusa, K. Ohkubo, M. Shiro and S. Fukuzumi, *Chem.–Eur. J.*, 2010, **16**, 3646.
13 (*a*) S. Fukuzumi, *Pure Appl. Chem.*, 2007, **79**, 981; (*b*) S. Fukuzumi, in *Functional Organic Materials*, ed. T. J. J. Müller and U. H. F. Bunz, Wiley-VCH, 2007, pp. 465–510.
14 (*a*) M. Brust, M. Walker, D. Bethell, D. J. Schiffrin and R. Whyman, *J. Chem. Soc., Chem. Commun.*, 1994, 801; (*b*) A. C. Templeton, W. P. Wuelfing and R. W. Murray, *Acc. Chem. Res.*, 2000, **33**, 27.
15 (*a*) C. A. Mirkin, R. L. Letsinger, R. C. Mucic and J. J. Storhoff, *Nature*, 1996, **382**, 607; (*b*) A. P. Alivisatos, K. P. Johnsson, X. Peng, T. E. Wilson, C. J. Loweth, M. P. Bruchez, Jr. and P. G. Schultz, *Nature*, 1996, **382**, 609; (*c*) R. Elghanian, J. J. Storhoff, R. C. Mucic, R. L. Letsinger and C. A. Mirkin, *Science*, 1997, **277**, 1078; (*d*) R. C. Mucic, J. J. Storhoff, C. A. Mirkin and R. L. Letsinger, *J. Am. Chem. Soc.*, 1998, **120**, 12674; (*e*) J. J. Storhoff and C. A. Mirkin, *Chem. Rev.*, 1999, **99**, 1849.
16 (*a*) P. D. Jadzinsky, G. Calero, C. J. Ackerson, D. A. Bushnell and R. D. Kornberg, *Science*, 2007, **318**, 430; (*b*) R. L. Whetten and R. C. Price, *Science*, 2007, **318**, 407.
17 P. V. Kamat, *J. Phys. Chem. C*, 2007, **111**, 2834.
18 (*a*) N. L. Rosi and C. A. Mirkin, *Chem. Rev.*, 2005, **105**, 1547; (*b*) R. Shenhar and V. M. Rotello, *Acc. Chem. Res.*, 2003, **36**, 549; (*c*) B.-C. Ye and B.-C. Yin, *Angew. Chem., Int. Ed.*, 2008, **47**, 8386.
19 (*a*) H. Imahori, M. Arimura, T. Hanada, Y. Nishimura, I. Yamazaki, Y. Sakata and S. Fukuzumi, *J. Am. Chem. Soc.*, 2001, **123**, 335; (*b*) H. Imahori, Y. Kashiwagi, Y. Endo, T. Hanada, Y. Nishimura, I. Yamazaki, Y. Araki, O. Ito and S. Fukuzumi, *Langmuir*, 2004, **20**, 73.
20 (*a*) D. K. Luttrull, A. A. Rehms, J. M. DeGraziano, X. C. Ma, F. Gao, R. E. Belford and T. T. Trier, *Science*, 1990, **248**, 199; (*b*) P. A. Liddell, G. Kodis, J. Andréasson, L. de la Garza, S. Bandyopadhyay, R. Mitchell, T. A. Moore, A. L. Moore and D. Gust, *J. Am. Chem. Soc.*, 2004, **126**, 4803; (*c*) Y. Terazono, G. Kodis, P. A. Liddell, V. Garg, T. A. Moore, A. L. Moore and D. Gust, *J. Phys. Chem. B*, 2009, **113**, 7147.
21 (*a*) S. Fukuzumi, H. Imahori, H. Yamada, M. E. El-Khouly, M. Fujitsuka, O. Ito and D. M. Guldi, *J. Am. Chem. Soc.*, 2001, **123**, 2571; (*b*) Y. Kobori, S. Yamauchi, K. Akiyama, S. Tero-Kubota, H. Imahori, S. Fukuzumi and J. R. Norris, *Proc. Natl. Acad. Sci. U. S. A.*, 2005, **102**, 10017; (*c*) F. D'Souza, C. A. Wijesinghe, M. E. El-Khouly, J. Hudson, M. Niemi, H. Lemmetyinen, N. V. Tkachenko, M. E. Zandler and S. Fukuzumi, *Phys. Chem. Chem. Phys.*, 2011, **13**, 18168.
22 (*a*) L. Sánchez, M. Sierra, N. Martín, A. J. Myles, T. J. Dale, Jr., J. Rebek, W. Seitz and D. M. Guldi, *Angew. Chem., Int. Ed.*, 2006, **45**, 4637; (*b*) M. S. Rodríguez-Morgade, M. E. Plonska-Brzezinska, A. J. Athans, E. Carbonell, G. de Miguel, D. M. Guldi, L. Echegoyen and T. Torres, *J. Am. Chem. Soc.*, 2009, **131**, 10484.
23 (*a*) H. Imahori, K. Tamaki, D. M. Guldi, C. Luo, M. Fujitsuka, O. Ito, Y. Sakata and S. Fukuzumi, *J. Am. Chem. Soc.*, 2001, **123**, 2607; (*b*) H. Imahori, D. M. Guldi, K. Tamaki, Y. Yoshida, C. Luo, Y. Sakata and S. Fukuzumi, *J. Am. Chem. Soc.*, 2001, **123**, 6617; (*c*) H. Imahori, K. Tamaki, Y. Araki, Y. Sekiguchi, O. Ito, Y. Sakata and S. Fukuzumi, *J. Am. Chem. Soc.*, 2002, **124**, 5165; (*d*) H. Imahori, Y. Sekiguchi, Y. Kashiwagi, T. Sato, Y. Araki, O. Ito, H. Yamada and S. Fukuzumi, *Chem.–Eur. J.*, 2004, **10**, 3184; (*e*) D. M. Guldi, H. Imahori, K. Tamaki, Y. Kashiwagi, H. Yamada, Y. Sakata and S. Fukuzumi, *J. Phys. Chem. A*, 2004, **108**, 541.
24 (*a*) D. Curiel, K. Ohkubo, J. R. Reimers, S. Fukuzumi and M. J. Crossley, *Phys. Chem. Chem. Phys.*, 2007, **9**, 5260; (*b*) J. A. Hutchison, P. J. Sintic, P. R. Brotherhood, C. Scholes, I. M. Blake, K. P. Ghiggino and M. J. Crossley, *J. Phys. Chem. C*, 2009, **113**, 11796; (*c*) J. A. Hutchison, P. J. Sintic, M. J. Crossley, T. Nagamura and K. P. Ghiggino, *Phys. Chem. Chem. Phys.*, 2009, **11**, 3478; (*d*) K. Ohkubo, P. J. Sintic, N. V. Tkachenko, H. Lemmetyinen, W. E, Z. Ou, J. Shao, K. M. Kadish, M. J. Crossley and S. Fukuzumi, *Chem. Phys.*, 2006, **326**, 3; (*e*) K. Ohkubo, R. Garcia, P. J. Sintic, T. Khoury, M. J. Crossley, K. M. Kadish and S. Fukuzumi, *Chem.–Eur. J.*, 2009, **15**, 10493; (*f*) S. H. Lee, A. G. Larsen, K. Ohkubo, J. R. Reimers, S. Fukuzumi and M. J. Crossley, *Chem. Sci.*, 2012, **3**, 257.
25 (*a*) C. A. Wijesinghe, M. E. El-Khouly, N. K. Subbaiyan, M. Supur, M. E. Zandler, K. Ohkubo, S. Fukuzumi and F. D'Souza, *Chem.–Eur. J.*, 2011, **17**, 3147; (*b*) A. Amin, M. E. El-Khouly, N. Subbaiyan, M. Zandler, M. Supur, S. Fukuzumi and F. D'Souza, *J. Phys. Chem. A*, 2011, **115**, 9810; (*c*) M. E. El-Khouly, D.-K. Ju, K.-Y. Kay, F. D'Souza and S. Fukuzumi, *Chem.–Eur. J.*, 2010, **16**, 6193.
26 (*a*) K. Ohkubo, H. Kotani, J. Shao, Z. Ou, K. M. Kadish, G. Li, R. K. Pandey, M. Fujitsuka, O. Ito, H. Imahori and S. Fukuzumi, *Angew. Chem., Int. Ed.*, 2004, **43**, 853; (*b*) Y. Kashiwagi, K. Ohkubo, J. A. MacDonald, I. M. Blake, M. J. Crossley, Y. Araki, O. Ito, H. Imahori and S. Fukuzumi, *Org. Lett.*, 2003, **5**, 2719; (*c*) S. Fukuzumi, K. Ohkubo, W. E, Z. Ou, J. Shao, K. M. Kadish, J. A. Hutchison, K. P. Ghiggino, P. J. Sintic and M. J. Crossley, *J. Am. Chem. Soc.*, 2003, **125**, 14984; (*d*) K. Ohkubo, H. Imahori, J. Shao, Z. Ou, K. M. Kadish, Y. Chen, G. Zheng, R. K. Pandey, M. Fujitsuka, O. Ito and S. Fukuzumi, *J. Phys. Chem. A*, 2002, **106**, 10991.
27 K. Ohkubo and S. Fukuzumi, *J. Porphyrins Phthalocyanines*, 2008, **12**, 993.
28 (*a*) M. Tanaka, K. Ohkubo, C. P. Gross, R. Guilard and S. Fukuzumi, *J. Am. Chem. Soc.*, 2006, **128**, 14625; (*b*) A. Takai, M. Chkounda, A. Eggenspiller, C. P. Gros, M. Lachkar, J.-M. Barbe and S. Fukuzumi, *J. Am. Chem. Soc.*, 2010, **132**, 4477.
29 Y. K. Kang, P. M. Iovine and M. J. Therien, *Coord. Chem. Rev.*, 2011, **255**, 804.
30 (*a*) R. Chitta, K. Ohkubo, M. Tasior, N. K. Subbaiyan, M. E. Zandler, D. T. Gryko, S. Fukuzumi and F. D'Souza, *J. Am. Chem. Soc.*, 2008, **130**, 14263; (*b*) J. L. Sessler, E. Karnas, S. K. Kim, Z. Ou, M. Zhang, K. M. Kadish, K. Ohkubo and S. Fukuzumi, *J. Am. Chem. Soc.*, 2008, **130**, 15256.
31 F. D'Souza, E. Maligaspe, K. Ohkubo, M. E. Zandler, N. K. Subbaiyan and S. Fukuzumi, *J. Am. Chem. Soc.*, 2009, **131**, 8787.
32 (*a*) M. Murakami, K. Ohkubo and S. Fukuzumi, *Chem.–Eur. J.*, 2010, **16**, 7820; (*b*) M. Murakami, K. Ohkubo, T. Nanjo, K. Souma, N. Suzuki and S. Fukuzumi, *ChemPhysChem*, 2010, **11**, 2594; (*c*) H. Sakai, H. Murata, M. Murakami, K. Ohkubo and S. Fukuzumi, *Appl. Phys. Lett.*, 2009, **95**, 252901.
33 (*a*) N. Mizoshita, K. Yamanaka, T. Shimada, T. Tani and S. Inagaki, *Chem. Commun.*, 2010, **46**, 9235; (*b*) S. Zilberg, *Phys. Chem. Chem. Phys.*, 2010, **12**, 10292.
34 S. Fukuzumi, H. Kotani, K. Ohkubo, S. Ogo, N. V. Tkachenko and H. Lemmetyinen, *J. Am. Chem. Soc.*, 2004, **126**, 1600.
35 A. Harriman, *Angew. Chem., Int. Ed.*, 2004, **43**, 4985.
36 S. Fukuzumi, R. Hanazaki, H. Kotani and K. Ohkubo, *J. Am. Chem. Soc.*, 2010, **132**, 11002.
37 T. Hasobe, S. Hattori, H. Kotani, K. Ohkubo, K. Hosomizu, H. Imahori, P. V. Kamat and S. Fukuzumi, *Org. Lett.*, 2004, **6**, 3103.
38 J. S. Moore and S. I. Stupp, *Macromolecules*, 1990, **23**, 65.
39 S. Fukuzumi, H. Kotani and K. Ohkubo, *Phys. Chem. Chem. Phys.*, 2008, **10**, 5159.
40 (*a*) A. C. Benniston, A. Harriman, P. Li, J. P. Rostron and J. W. Verhoeven, *Chem. Commun.*, 2005, 2701; (*b*) A. C. Benniston, A. Harriman, P. Li, J. P. Rostron, H. J. van Ramesdonk, M. M. Groeneveld, H. Zhang and J. W. Verhoeven, *J. Am. Chem. Soc.*, 2005, **127**, 16054; (*c*) A. C. Benniston,

A. Harriman and J. W. Verhoeven, *Phys. Chem. Chem. Phys.*, 2008, **10**, 5156.
41 H. van Willigen, G. Jones, II and M. S. Farahat, *J. Phys. Chem.*, 1996, **100**, 3312.
42 Y. Yamada, T. Miyahigashi, H. Kotani, K. Ohkubo and S. Fukuzumi, *J. Am. Chem. Soc.*, 2011, **133**, 16136.
43 H. Kotani, K. Ohkubo and S. Fukuzumi, *Faraday Discuss.*, 2012, **155**, DOI: 10.1039/c1fd00084e.
44 (*a*) S. V. Rosokha, M. D. Newton, A. S. Jalilov and J. K. Kochi, *J. Am. Chem. Soc.*, 2008, **130**, 1944; (*b*) S. V. Rosokha and J. K. Kochi, *J. Am. Chem. Soc.*, 2007, **129**, 3683; (*c*) D.-L. Sun, S. V. Rosokha and J. K. Kochi, *J. Am. Chem. Soc.*, 2004, **126**, 1388; (*d*) K. Ohkubo, T. Kobayshi and S. Fukuzumi, *Angew. Chem., Int. Ed.*, 2011, **50**, 8652.
45 (*a*) A. Takai, C. P. Gros, R. Guilard and S. Fukuzumi, *Chem.–Eur. J.*, 2009, **15**, 3110–3122; (*b*) A. Takai, C. P. Gros, J.-M. Barbe and S. Fukuzumi, *Phys. Chem. Chem. Phys.*, 2010, **12**, 12160; (*c*) A. Takai, C. P. Gros, J.-M. Barbe and S. Fukuzumi, *Chem.–Eur. J.*, 2011, **17**, 3420.
46 J. S. Park, E. Karnas, K. Ohkubo, P. Chen, K. M. Kadish, S. Fukuzumi, C. Bielawski, T. W. Hudnall, V. M. Lynch and J. L. Sessler, *Science*, 2010, **329**, 1324.
47 K. Ohkubo, H. Kotani and S. Fukuzumi, *Chem. Commun.*, 2005, 4520.
48 O. Morawski and J. Prochorow, *Chem. Phys. Lett.*, 1995, **242**, 253.
49 (*a*) K. Kikuchi, C. Sato, M. Watabe, H. Ikeda, Y. Takahashi and T. Miyashi, *J. Am. Chem. Soc.*, 1993, **115**, 5180; (*b*) K. Kasama, K. Kikuchi, Y. Nishida and H. Kokubun, *J. Phys. Chem.*, 1981, **85**, 4148.
50 K. Ohkubo and S. Fukuzumi, *Bull. Chem. Soc. Jpn.*, 2009, **82**, 303.
51 (*a*) K. Ohkubo, T. Nanjo and S. Fukuzumi, *Bull. Chem. Soc. Jpn.*, 2006, **79**, 1489; (*b*) H. Kotani, K. Ohkubo and S. Fukuzumi, *J. Am. Chem. Soc.*, 2004, **126**, 15999; (*c*) K. Ohkubo, T. Nanjo and S. Fukuzumi, *Org. Lett.*, 2005, **7**, 4265; (*d*) K. Ohkubo, T. Nanjo and S. Fukuzumi, *Catal. Today*, 2006, **117**, 356; (*e*) K. Ohkubo, A. Fujimoto and S. Fukuzumi, *Chem. Commun.*, 2011, **47**, 8515.
52 (*a*) K. Ohkubo, K. Yukimoto and S. Fukuzumi, *Chem. Commun.*, 2006, 2504; (*b*) M. Tanaka, K. Yukimoto, K. Ohkubo and S. Fukuzumi, *J. Photochem. Photobiol., A*, 2008, **197**, 206.
53 (*a*) K. Ohkubo, K. Mizushima, R. Iwata, K. Souma, N. Suzuki and S. Fukuzumi, *Chem. Commun.*, 2010, **46**, 601; (*b*) H. Kotani, K. Ohkubo and S. Fukuzumi, *Appl. Catal., B*, 2008, **77**, 317.
54 (*a*) K. Ohkubo, K. Mizushima, R. Iwata and S. Fukuzumi, *Chem. Sci.*, 2011, **2**, 715; (*b*) K. Ohkubo, K. Mizushima and S. Fukuzumi, *Res. Chem. Intermed.*, 2011, in press.
55 K. Ohkubo, R. Iwata, T. Yanagimoto and S. Fukuzumi, *Chem. Commun.*, 2007, 3139.
56 K. Ohkubo, R. Iwata, S. Miyazaki, T. Kojima and S. Fukuzumi, *Org. Lett.*, 2006, **8**, 6079.
57 T. Hasobe, S. Hattori, P. V. Kamat, Y. Wada and S. Fukuzumi, *J. Mater. Chem.*, 2005, **15**, 372.
58 T. Hasobe, H. Imahori, S. Fukuzumi and P. V. Kamat, *J. Phys. Chem. B*, 2003, **107**, 12105.
59 D. R. Lawson, D. L. Feldheim, C. A. Foss, P. K. Dorhout, C. M. Elliott, C. R. Martin and B. Parkinson, *J. Electrochem. Soc.*, 1992, **139**, L68.
60 S. Fukuzumi, T. Suenobu, M. Patz, T. Hirasaka, S. Itoh, M. Fujitsuka and O. Ito, *J. Am. Chem. Soc.*, 1998, **120**, 8060.
61 S. Fukuzumi, Y. Yamada, T. Suenobu, K. Ohkubo and H. Kotani, *Energy Environ. Sci.*, 2011, **4**, 2754.
62 J. R. Darwent, P. Douglas, A. Harriman, G. Porter and M.-C. Richoux, *Coord. Chem. Rev.*, 1982, **44**, 83.
63 J. Kiwi, Kalyanasundram and M. Grätzel, *Struct. Bonding*, 1982, **49**, 37.
64 (*a*) I. Okura, *Coord. Chem. Rev.*, 1985, **68**, 53; (*b*) I. Okura, *Photosensitization of Porphyrins and Phthalocyanines*, Kodansha, Tokyo, 2000; (*c*) Y. Amao and I. Okura, *J. Mol. Catal. B: Enzym.*, 2002, **17**, 9; (*d*) I. Okura and H. Hosono, *J. Phys. Chem.*, 1992, **96**, 4466.
65 (*a*) D.-L. Jiang, C.-K. Choi, K. Honda, W.-S. Li, T. Yuzawa and T. Aida, *J. Am. Chem. Soc.*, 2004, **126**, 12084; (*b*) N. Himeshima and Y. Amao, *Energy Fuels*, 2003, **17**, 1641; (*c*) Y. Astuti, E. Palomares, S. A. Haque and J. R. Durrant, *J. Am. Chem. Soc.*, 2005, **127**, 15120.
66 H. Kotani, T. Ono, K. Ohkubo and S. Fukuzumi, *Phys. Chem. Chem. Phys.*, 2007, **9**, 1487.
67 H. Kotani, R. Hanazaki, K. Ohkubo, Y. Yamada and S. Fukuzumi, *Chem.–Eur. J.*, 2011, **17**, 2777.
68 H. Kotani, K. Ohkubo, Y. Takai and S. Fukuzumi, *J. Phys. Chem. B*, 2006, **110**, 24047.
69 (*a*) A. C. Templeton, D. E. Cliffel and R. W. Murray, *J. Am. Chem. Soc.*, 1999, **121**, 7081; (*b*) D. E. Cliffel, F. P. Zamborini, S. M. Gross and R. W. Murray, *Langmuir*, 2000, **16**, 9699.
70 (*a*) S. E. Eklund and D. E. Cliffel, *Langmuir*, 2004, **20**, 6012; (*b*) S. Chen and K. Kimura, *J. Phys. Chem. B*, 2001, **105**, 5397; (*c*) Y. Li, J. Petroski and M. A. El-Sayed, *J. Phys. Chem. B*, 2000, **104**, 10956.
71 X.-Q. Zhu, Y. Yang, M. Zhang and J.-P. Cheng, *J. Am. Chem. Soc.*, 2003, **125**, 15298.
72 S. Fukuzumi and T. Tanaka, in *Photoinduced Electron Transfer*, ed. M. A. Fox and M. Chanon, Elsevier, Amsterdam, 1988, Part C, Chap. 10.
73 H. Imahori, Y. Kashiwagi, T. Hanada, Y. Endo, Y. Nishimura, I. Yamazaki and S. Fukuzumi, *J. Mater. Chem.*, 2003, **13**, 2890.
74 H. Imahori, H. Norieda, Y. Nishimura, I. Yamazaki, K. Higuchi, N. Kato, T. Motohiro, H. Yamada, T. Tamaki, M. Arimura and Y. Sakata, *J. Phys. Chem. B*, 2000, **104**, 1253.
75 (*a*) M. Mandal, S. Kumar Ghosh, S. Kundu, K. Esumi and T. Pal, *Langmuir*, 2002, **18**, 7792; (*b*) H. Yao, O. Momozawa, T. Hamatani and K. Kimura, *Chem. Mater.*, 2001, **13**, 4692.
76 F. P. Zamborini, S. M. Gross and R. W. Murray, *Langmuir*, 2001, **17**, 481.
77 M. J. Hostetler, C.-J. Zhong, B. K. H. Yen, J. Anderegg, S. M. Gross, N. D. Evans, M. Porter and R. W. Murray, *J. Am. Chem. Soc.*, 1998, **120**, 9396.
78 S. Fukuzumi, Y. Endo, Y. Kashiwagi, Y. Araki, O. Ito and H. Imahori, *J. Phys. Chem. B*, 2003, **107**, 11979.
79 (*a*) T. Hasobe, H. Imahori, S. Fukuzumi and P. V. Kamat, *J. Am. Chem. Soc.*, 2003, **125**, 14962; (*b*) T. Hasobe, H. Imahori, P. V. Kamat, T. K. Ahn, S. K. Kim, D. Kim, A. Fujimoto, T. Hirakawa and S. Fukuzumi, *J. Am. Chem. Soc.*, 2005, **127**, 1216.
80 A. Bar-Haim, J. Klafter and R. Kopelman, *J. Am. Chem. Soc.*, 1997, **119**, 6197.
81 (*a*) E. K. L. Yeow, K. P. Ghiggino, J. N. H. Reek, M. J. Crossley, A. W. Bosman, A. P. H. J. Schenning and E. W. Meijer, *J. Phys. Chem. B*, 2000, **104**, 2596; (*b*) S. L. Gilat, A. Adronov and J. M. J. Frechet, *Angew. Chem., Int. Ed.*, 1999, **38**, 1422.
82 (*a*) W.-S. Li and T. Aida, *Chem. Rev.*, 2009, **109**, 6047; (*b*) D.-L. Jiang and T. Aida, *J. Am. Chem. Soc.*, 1998, **120**, 10895.
83 C.-Y. Huang and Y. O. Su, *Dalton Trans.*, 2010, **39**, 8306.
84 T. Hasobe, Y. Kashiwagi, M. A. Absalom, J. Sly, K. Hosomizu, M. J. Crossley, H. Imahori, P. V. Kamat and S. Fukuzumi, *Adv. Mater.*, 2004, **16**, 975.
85 F. D'Souza, G. R. Deviprasad, M. E. Zandler, V. T. Hoang, A. Klykov, M. VanStipdonk, A. Perera, M. E. El-Khouly, M. Fujitsuka and O. Ito, *J. Phys. Chem. A*, 2002, **106**, 3243.
86 T. Hasobe, P. V. Kamat, M. A. Absalom, Y. Kashiwagi, J. Sly, M. J. Crossley, K. Hosomizu, H. Imahori and S. Fukuzumi, *J. Phys. Chem. B*, 2004, **108**, 12865.
87 (*a*) N. Solladié, A. Hamel and M. Gross, *Tetrahedron Lett.*, 2000, **41**, 6075; (*b*) F. Aziat, R. Rein, J. Peon, E. Rivera and N. Solladié, *J. Porphyrins Phthalocyanines*, 2008, **12**, 1232.
88 (*a*) M. Fujitsuka, M. Hara, S. Tojo, A. Okada, V. Troiani, N. Solladié and T. Majima, *J. Phys. Chem. B*, 2005, **109**, 33; (*b*) M. Fujitsuka, D. W. Cho, N. Solladié, V. Troiani, H. Qiu and T. Majima, *J. Photochem. Photobiol., A*, 2007, **188**, 346.
89 K. Saito, V. Troiani, H. Qiu, N. Solladié, T. Sakata, H. Mori, M. Ohama and S. Fukuzumi, *J. Phys. Chem. C*, 2007, **111**, 1194.
90 F. D'Souza, P. M. Smith, S. Gadde, A. L. McCarty, M. J. Kullman, M. E. Zandler, M. Itou, Y. Araki and O. Ito, *J. Phys. Chem. B*, 2004, **108**, 11333.
91 F. D'Souza, G. R. Deviprasad, M. S. Rahman and J.-P. Choi, *Inorg. Chem.*, 1999, **38**, 2157.
92 S. Fukuzumi, K. Saito, K. Ohkubo, V. Troiani, H. Qiu, S. Gadde, F. D'Souza and N. Solladié, *Phys. Chem. Chem. Phys.*, 2011, **13**, 17019.
93 (*a*) T. Hasobe, P. V. Kamat, V. Troiani, N. Solladié, T. K. Ahn, S. K. Kim, D. Kim, A. Kongkanand, S. Kuwabata and S. Fukuzumi, *J. Phys. Chem. B*, 2005, **109**, 19; (*b*) T. Hasobe,

K. Saito, P. V. Kamat, V. Troiani, H. Qiu, N. Solladié, K. S. Kim, J. K. Park, D. Kim, F. D'Souza and S. Fukuzumi, *J. Mater. Chem.*, 2007, **17**, 4160.
94 S. Iijima, *Nature*, 1991, **354**, 56.
95 (*a*) *Carbon Nanotubes and Related Structures: Synthesis, Characterization, Functionalization, and Applications*, ed. D. M. Guldi and N. Martin, Wiley-VCH Verlag GmbH & Co. KGaA, 2010; (*b*) P. J. F. Harris, *Carbon Nanotubes and Related Structures-New Materials for the Twenty-First Century*, Cambridge University Press, Cambridge, U.K., 2001; (*c*) Y. Ma, B. Wang, Y. Wu, Y. Huang and Y. Chen, *Carbon*, 2011, **49**, 4098; (*d*) W. Zhou, L. Ding, S. Yang and J. Liu, *J. Am. Chem. Soc.*, 2010, **132**, 336.
96 (*a*) P. Avouris, *Acc. Chem. Res.*, 2002, **35**, 1026; (*b*) V. Sgobba and D. M. Guldi, *J. Mater. Chem.*, 2008, **18**, 153.
97 (*a*) J. M. Schnorr and T. M. Swager, *Chem. Mater.*, 2011, **23**, 646; (*b*) J. H. Bitter, *J. Mater. Chem.*, 2010, **20**, 7312; (*c*) B. K. Gorityala, J. Ma, X. Wang, P. Chen and X.-W. Liu, *Chem. Soc. Rev.*, 2010, **39**, 2925.
98 M. J. O'Connell, S. M. Bachilo, C. B. Huffman, V. C. Moore, M. S. Strano, E. H. Haroz, K. L. Rialon, P. J. Boul, W. H. Noon, C. Kittrell, J. P. Ma, R. H. Hauge, R. B. Weisman and R. E. Smalley, *Science*, 2002, **297**, 593.
99 J. A. Misewich, R. Martel, P. Avouris, J. C. Tsang, S. Heinze and J. Tersoff, *Science*, 2003, **300**, 783.
100 (*a*) S. Nigoyi, M. A. Hamon, H. Hu, B. Zhao, P. Bhomwik, R. Sen, M. E. Itkis and R. C. Haddon, *Acc. Chem. Res.*, 2002, **35**, 1105; (*b*) Y.-P. Sun, K. Fu, Y. Lin and W. Huang, *Acc. Chem. Res.*, 2002, **35**, 1096.
101 (*a*) A. Hirsch, *Angew. Chem., Int. Ed.*, 2002, **41**, 1853; (*b*) J. L. Barh and J. M. Tour, *J. Mater. Chem.*, 2002, **12**, 1952; (*c*) S. Banerjee, M. G. C. Kahn and S. S. Wong, *Chem.–Eur. J.*, 2003, **9**, 1898.
102 (*a*) D. Tasis, N. Tagmatarchis, V. Georgakilas and M. Prato, *Chem.–Eur. J.*, 2003, **9**, 4001; (*b*) C. A. Dyke and J. M. Tour, *Chem.–Eur. J.*, 2004, **10**, 812; (*c*) S. Banerjee, T. Hemraj-Benny and S. S. Wong, *Adv. Mater.*, 2005, **17**, 17; (*d*) D. Tasis, N. Tagmatarchis and A. Bianco, *Chem. Rev.*, 2006, **106**, 1105; (*e*) R. Chitta and F. D'Souza, *J. Mater. Chem.*, 2008, **18**, 1440.
103 (*a*) D. M. Guldi, *J. Phys. Chem. B*, 2005, **109**, 11432; (*b*) D. M. Guldi, *Phys. Chem. Chem. Phys.*, 2007, 1400; (*c*) D. M. Guldi, G. M. A. Rahman, V. Sgobba and C. Ehli, *Chem. Soc. Rev.*, 2006, **35**, 471.
104 D. M. Guldi and V. Sgobba, *Chem. Commun.*, 2011, **47**, 606.
105 D. Baskaran, J. M. Mays, X. P. Zhang and M. S. Bratcher, *J. Am. Chem. Soc.*, 2005, **127**, 6916.
106 F. D'Souza, A. S. D. Sandanayaka and O. Ito, *J. Phys. Chem. Lett.*, 2010, **1**, 2586.
107 C. Oelsner, C. Schmidt, F. Hauke, M. Prato, A. Hirsch and D. M. Guldi, *J. Am. Chem. Soc.*, 2011, **133**, 4580.
108 (*a*) M. Ohtani and S. Fukuzumi, *Chem. Commun.*, 2009, 4997; (*b*) M. Ohtani, P. V. Kamat and S. Fukuzumi, *J. Mater. Chem.*, 2010, **20**, 582.
109 (*a*) S. M. Bachilo, L. Balzano, J. E. Herrera, F. Pompeo, D. E. Resasco and R. B. Weisman, *J. Am. Chem. Soc.*, 2003, **125**, 11186; (*b*) K. Hata, D. N. Futaba, K. Mizuno, T. Namai, M. Yumura and S. Iijima, *Science*, 2004, **306**, 1362.
110 (*a*) D. Chattopadhyay, S. Lastella, S. Kim and F. Papadimitrakopoulos, *J. Am. Chem. Soc.*, 2002, **124**, 728; (*b*) D. A. Heller, R. M. Mayrhofer, S. Baik, Y. V. Grinkova, M. L. Usrey and M. S. Strano, *J. Am. Chem. Soc.*, 2004, **126**, 14567.
111 M. Endo, Y. A. Kim, T. Hayashi, Y. Fukai, K. Oshida, M. Terrones, T. Yanagisawa, S. Higaki and M. S. Dresselhaus, *Appl. Phys. Lett.*, 2002, **80**, 1267.
112 (*a*) C. Kim, Y. J. Kim, Y. A. Kim, T. Yanagisawa, K. C. Park, M. Endo and M. S. Dresselhaus, *J. Appl. Phys.*, 2004, **96**, 5903; (*b*) M. Endo, Y. A. Kim, M. Ezaka, K. Osada, T. Yanagisawa, T. Hayashi, M. Terrones and M. S. Dresselhaus, *Nano Lett.*, 2003, **3**, 723.
113 T. Hasobe, S. Fukuzumi and P. V. Kamat, *Angew. Chem., Int. Ed.*, 2006, **45**, 755.
114 (*a*) T. Hasobe, S. Fukuzumi and P. V. Kamat, *J. Phys. Chem. B*, 2006, **110**, 25477; (*b*) R. Chitta, A. S. D. Sandanayaka, A. L. Schmacher, L. D'Souza, Y. Araki, O. Ito and F. D'Souza, *J. Phys. Chem. C*, 2007, **111**, 6947.
115 K. Saito, M. Ohtani, T. Sakata, H. Mori and S. Fukuzumi, *J. Am. Chem. Soc.*, 2006, **128**, 14216.
116 K. Saito, M. Ohtani and S. Fukuzumi, *Chem. Commun.*, 2007, 55.
117 M. Ohtani, K. Saito and S. Fukuzumi, *Chem.–Eur. J.*, 2009, **15**, 9160.
118 (*a*) M. S. Dresselhaus, G. Dresselhaus and A. Jorio, *J. Phys. Chem. C*, 2007, **111**, 17887; (*b*) Z. Yu and L. Brus, *J. Phys. Chem. B*, 2001, **105**, 1123; (*c*) J. Kürti, V. Zólyomi, A. Grüneis and H. Kuzmany, *Phys. Rev. B: Condens. Matter*, 2002, **65**, 165433; (*d*) M. S. Dresselhaus, G. Dresselhaus, R. Saito and A. Jorio, *Phys. Rep.*, 2005, **409**, 47.
119 (*a*) M. Ohtani and S. Fukuzumi, *J. Porphyrins Phthalocyanines*, 2010, **14**, 452; (*b*) M. Ohtani and S. Fukuzumi, *Fullerenes, Nanotubes, Carbon Nanostruct.*, 2010, **18**, 251.